Journal of Chromatography B, 878 (2010) 2693–2700

Contents lists available at ScienceDirect

Journal of Chromatography B

journal homepage: www.elsevier.com/locate/chromb

Isolation of lignans from *Schisandra chinensis* with anti-proliferative activity in human colorectal carcinoma: Structure–activity relationships

John Gnabre[a,b], Irem Unlu[a,1], Tso-cheng Chang[b], Paul Lisseck[b], Bryan Bourne[c], Ryan Scolnik[c], Neil E. Jacobsen[c], Robert Bates[c], Ru Chih Huang[a,*]

[a] Department of Biology, Johns Hopkins University, Mudd Hall, 3400 N. Charles Street, Baltimore, MD 21218, USA
[b] Dr. Chang Naturals, LLC, P.O. Box 191, South Deerfield, MA 01373, USA
[c] Department of Chemistry, University of Arizona, 1306 E. University Blvd, Tucson, AZ 85721, USA

ARTICLE INFO

Article history:
Received 3 June 2010
Accepted 6 August 2010
Available online 14 August 2010

Keywords:
Schisandra chinensis
Lignans
Anti-proliferation
Automated repeat-injection
Conformation

ABSTRACT

Separate benzocyclooctadiene lignans were isolated from the berries of *Schisandra chinensis* in milligram quantities on analytical reverse phase (RP) HPLC by an automated repeat-injection method and shown to have anti-proliferative activity against human colorectal cancer cells. Structures of the compounds were determined by a combination of NMR and mass spectrometry. Stereospecific NMR assignments for gomisin-N and deoxyschisandrin, gave more complete and accurate data than previously reported, based on 600 MHz 2D HSQC, DQF-COSY and HMBC data. Comparison of coupling constants and HMBC crosspeak intensities with calculated and X-ray crystal structures confirmed their stereochemistry and conformation. Analysis of structure–activity relationships revealed the importance of key structural determinants. The *S*-biphenyl configuration of gomisin N, the most active lignan, correlated with increased anti-proliferative activity, while the presence of a hydroxyl group at the C7 position reduced or abolished this activity. Increased activity was also observed when a methylenedioxy group was present between C12 and C13. The percent yield of the most active compounds relative to the starting plant materials was 0.0156% for deoxyschisandrin and 0.0173% for gomisin N. The results of these studies indicate that automated repeat-injection method of analytical HPLC may provide a superior alternative to the standard semi-preparative HPLC techniques for separation of complex mixtures.

1. Introduction

The berry-bearing creeping vine *Schisandra chinensis* (Turcz.) Baill. (Schisandraceae or Magnoliaceae), commonly known as lemonwood, Chinese mock-barberry or 'Chinese Magnolia', is a popular medicinal plant endemic to the eastern regions of China, Japan, Korea and far east of Russia [1].

Today the product continues to be the subject of research interest to Asian scientists in areas such as diseases of the liver, digestive tract, lungs and kidneys. In Russia, Schisandra is a registered medicine for vision problems. In Chinese and Japanese traditional medicine, the dried ripe berries have been used for thousands of years for human ailments as varied as chronic cough, shortness of breath, inflammation, insomnia, diabetes, coronary heart disease, skin disorders, depression and menopausal symptoms [2,3]. Schisandra species, especially, *S. chinensis* and *S. sphenanthera*, have been intensively investigated [4].

Lignans are major constituents of these plants and are responsible for the myriad of activities ascribed to fruit extracts. The first dibenzocyclooctadiene lignan isolated from the fruit of *S. chinensis* dates back to 1961 and was termed schisandrin [5] or gomisin in Japan. Recent advances in analytical techniques have enabled a more comprehensive characterization of the lignans of these two schisandra species. Over 50 constituents have been identified and categorized into five classes from type A to type E [4]. The most abundant class, the dibenzocyclooctadiene lignans (type A), makes up over 80% of the lignans in the fruit of *S. chinensis*. A growing body of evidence associates these lignans with pro-apoptotic and tumor-suppressing activities [6–9].

Schisandra ripe berries have also been shown to be rich in phytoestrogens, minerals, vitamins and essential oils [10]. These chemical contents may be responsible for the pungent, sour, sweet, salty and bitter taste, hence its Chinese denotation of *wǔ wèi zi* or 'five flavor fruit'. Schisandra berries have been known in the U.S. since the 1950s, sold mostly in natural food stores in extract form. Until recently all Schisandra berries were imported from China.

* Corresponding author. Tel.: +1 410 516 7314; fax: +1 410 516 5213.
E-mail address: rhuang@jhu.edu (R.C. Huang).
[1] Department of Molecular Biology and Genetics, KP 301, Boğaziçi University, Bebek, 34342 Istanbul, Turkey.

1570-0232/$ – see front matter © 2010 Elsevier B.V. All rights reserved.
doi:10.1016/j.jchromb.2010.08.005

Now U.S. grower (Dr. TT Chang) offers certified-organic Schisandra in several quick-frozen formats. The comestible use of the fruit products and the increasing evidence of its anticancer properties prompted the current investigation as to whether the active constituents could stop colon cancer. The robust MTS cell viability assay with the p53-mutant human colon HT-29 cell line served as an assay-guided screening tool for the purification of the active principles of the fruit extract.

Compound purity is critical in the paradigm of drug discovery. Therefore, more and more analytical laboratories have been combining state-of-the-art automated analytical instrumentations with high throughput screening to achieve high efficiency in drug discovery [11]. Thus, a number of analytical methods have been used to resolve the constituents of the extracts of Schisandra berries but with varying with degrees of success [4]. More recently, tandem HPLC/mass spectrometry and NMR was applied to the separation and characterization of a large number of Schisandra fruit components [12]. However, very few analytical separation techniques have been able to generate substantial amounts of pure compounds for pharmacological evaluation [4,13].

The current studies take advantage of the progress in the automation of the separation techniques enabled by the flexibility of analytical HPLC interfaces. Thus, pure benzocyclooctadiene lignans contained in Schisandra berry crude extract were separated in a single run on a reversed phase analytical HPLC due to the high number of theoretical plates provided by the analytical scale column. Conditions were optimized in order to achieve a reproducible separation over a period of 48–96 h, allowing separation of 1–20 mg of pure compounds by multiple consecutive injection/collection cycles. In this report, we propose a cost-effective and highly efficient strategy superior to the standard semi-preparative HPLC.

2. Materials and methods

2.1. Reagents

2.1.1. Plant materials

Frozen ripe berries of *Schisandra chinensis* were a gift of Zana Products – Dr. Chang Naturals, LLC of, P.O. Box 191, South Deerfield, MA 01373, USA (www.organicchiberry.com). Two batches of the plant specimens were collected and shipped at different seasons. Batch I was received in October 2007 and batch II in February 2009. The berries were shipped frozen and upon arrival, were immediately thawed and placed in a 45 °C oven for several days until they were dry. The materials were then ground into a powder in a Coffee Mill blender, and the benzocyclooctadiene lignans were extracted following the scheme outlined in Fig. 1. All fractions generated by subsequent HPLC studies were dried in a SpeedVac (Savant Instruments Inc., Holbrook, NY) weighed and monitored by silica gel thin-layer chromatography (TLC) with cerium sulfate charring [2% $CeSO_4$ (w/v) in 5.6% H_2SO_4 (v/v)]. For testing in cell culture, all dried test materials were solubilized at 100 mg/ml or 100 mM in dimethylsulfoxide (DMSO) to give stock solutions which were stored at −20 °C.

2.1.2. HPLC reagents and instruments

Acetonitrile (MeCN) and glacial acetic acid were purchased from J.T. Baker (Phillipsburg, NJ, USA). HPLC grade water was purchased from Fisher Scientific (Fair Lawn, NJ, USA). The fractionation of the plant extracts was performed using a Waters 2695 Separations Module (Waters Associates, Milford, MA) equipped with a Waters 2996 photodiode array detector (PDA), a Waters fraction collector II, and an Atlantis dC18 reversed phase column (4.6 mm × 150 mm, 3 μm particle size, Part No. 18800-1342, Waters) maintained at 35 °C. The system was controlled by an Empower 2 chromatography manager (Waters). The PDA detector was operated between 200 and 400 nm, and qualitative profile chromatograms were extracted at 220 nm.

2.1.3. Cell lines

Erythroleukemia K562, human colon HT-29 and breast MCF-7 cancer cell lines were obtained from the American Type Culture Collection (Manassas, VA, USA). All cells were maintained in Dulbecco's modified Eagle's medium (DMEM) supplemented with 10% fetal bovine serum, penicillin (100 U ml^{-1}) and streptomycin (100 U ml^{-1}). Cells were incubated at 37 °C in a 5% CO_2 humidified atmosphere.

2.2. MTS cell viability assay

Cells were seeded at a density of 1.5×10^4 cells/well in a 96-well plate. When the cells reached 60–70% confluency, the growth medium was aspirated and the wells were rinsed with pre-warmed PBS. Test compounds at various concentrations or 1% DMSO (vehicle control) were then added and the plates were incubated for 72 h. After incubation, 40 μl of a solution of CellTiter 96 Aqueous One Solution (Promega, Madison, WI, USA) containing MTS [3-(4,5-dimethylthiazol-2-yl)-5-(3-carboxymethoxyphenyl)-2-(4-sulfophenyl)-2H-tetrazolium)] and an electron coupling reagent (phenazine ethosulfate) were added to each well with an auto-repeat pipetor. The plates were incubated for 3 h during which time the reagent was bio-reduced into a colored formazan product by the intracellular dehydrogenase enzymes of metabolically active cells. The quantity of formazan produced is directly proportional to the number of living cells in the cultures. The absorbance (A) was measured at 490 nm (reference at 690 nm) on a PowerWave 200 microplate reader (Bio-Tek Instruments). The results were expressed as percent cell viability, calculated for each drug concentration using the formula:

$$\%\,\text{Viability} = \left(\frac{A_{\text{treated group}}}{A_{\text{control group}}}\right) \times 100.$$

100% viability was represented by samples with the DMSO vehicle control.

The IC_{50} values were obtained from the sigmoidal curve by plotting the percentage viability of cells against the drug concentration using Psi-Plot version 9, Poly Software International (Pearl River, NY, USA).

2.3. NMR experimental

NMR spectra were acquired at 25 °C using a Bruker DRX-600 spectrometer with a Nalorac 5 mm inverse H/C/N probe with a z-axis gradient. 2D DQF-COSY, edited decoupled HSQC and magnitude mode HMBC experiments used standard Bruker pulse sequences. All 2D acquisitions used 750 t_1 increments and data were zero-filled to give a 2048 (F_2) × 1024 (F_1) point 2D matrix. NMR data was processed and analyzed using the Felix software package. 3D molecular modeling and energy minimization were performed using the Insight II (Accelerys, Inc.) software package.

3. Results and discussion

3.1. Anti-proliferative activity of dichloromethane extracts of S. chinensis in cancer cells

The dichloromethane (DCM) extracts of Schisandra dry berries were initially compared by TLC to establish whether the season of collection had some influence on the contents of active principles. The results revealed no significant difference. However, the

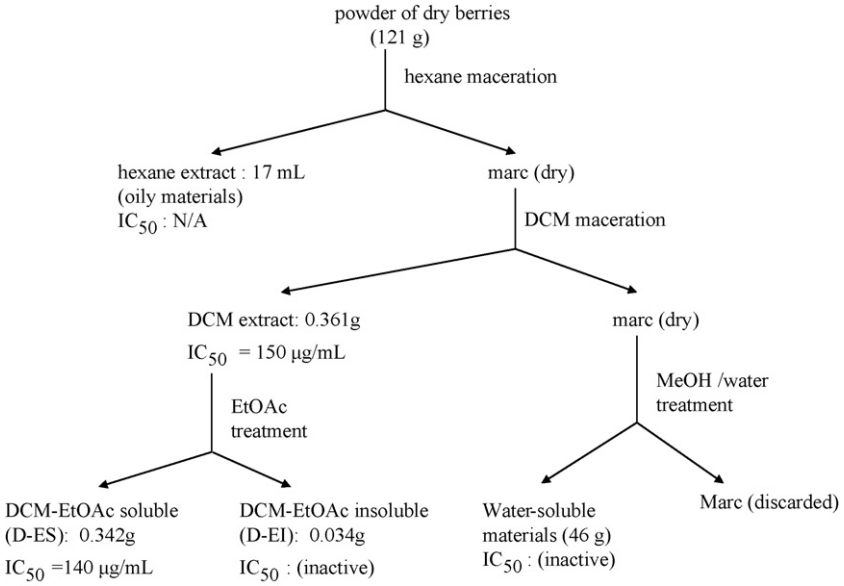

Fig. 1. Scheme of assay-guided differential fractionation of the dry berries of *S. chinensis*. Powder of the berries was initially defatted with hexane and the marc was macerated with dichloromethane (DCM) to generate an active DCM extract. Further treatment of the DCM-exhausted marc by 50% methanol yielded inactive water soluble materials. Plant extracts were tested stepwise for anti-proliferative activity against the human colorectal carcinoma cell line HT29, as described in Section 2.

fall batch appeared to be slightly richer in plant constituents than the winter batch, as assessed by TLC. The activity of the two batches was then assessed on three common cancer cell lines at a concentration varying from 1 to 100 μg/ml to determine whether the active constituents had specificity against a particular cancer cell type. The results (not shown) consistently revealed that the ingredients of the DCM extracts of the two batches had strong activity against human colon HT-29, but no detectable activity against erythroleukemia K562, and only weak activity against human breast MCF-7. There was no significant difference between the two batches. Based on these results, the HT-29 cell line was used as a target for the fractionation and isolation of the anti-proliferative activity of the two batches of Schisandra berries.

3.2. Differential fractionation of the powder of Schisandra berries

Powder of Schisandra dried berries was macerated with hexane and the marc was then extracted by bioassay-guided differential fractionation (Fig. 1).

The dichloromethane/ethyl acetate (DCM–EtOAc) soluble materials (D-ES) were dried and further defatted with hexane to yield a working extract referred to as total hexane insoluble materials (THIM) which was used in the HPLC studies. All extracts were analyzed by TLC and stepwise tested for inhibition of human carcinoma HT-29 cell growth as described in Section 2.2. Although thoroughly defatted, the IC_{50} of THIM (136 μg/ml) was not significantly different from that of D-ES (140 μg/ml).

3.3. Fractionation by HPLC of the first batch of THIM extract

The separation of the first batch of THIM extract was performed using a gradient of 0.1% acetic acid in acetonitrile (solvent B) and 0.1% acetic acid in water (solvent A) and the flow rate set at 1.0 ml/min. The elution gradient was from 55% to 100% solvent B over 50 min with the non-linear gradient curve 7. The column was cleaned 15 min with 100% solvent B and re-equilibrated for 10 min before the following injection. About 20 mg of the plant extract (THIM) was dissolved in 4 ml of acetone/hexane (5 mg/ml). The injection volume was fixed at 30 μl, resulting in about 150 μg of sample injected in the column for each injection. The sample was injected about 40 consecutive times and the collection was achieved using a Waters Fraction Collector II. A blank run preceded each collection procedure. The automated injection/collection cycles were repeated over a 48-h period with the partial overlay shown in Fig. 2. All fractions were dry, weighed, analyzed by TLC with cerium sulfate charring and the targeted peaks (T1 to T5) were tested for biological activity.

The full chromatogram shows a peak cluster (not shown) eluting in the first 8 min and devoid of detectable activity. However, another cluster eluting from the 17th to the 28th minute (not shown) was active but much less than the parent THIM extract. Furthermore, the cluster was still relatively complex with no outstanding peak. These factors discouraged further separation. The chemical structure was determined by NMR/mass spectrometry. The degree of purity of each peak was determined by tandem HPLC/NMR under the conditions described in Section 2 for the NMR, and found to be >90%. The overlay of the chromatograms in Fig. 2 reflects the reproducibility of the analytical reverse phase HPLC method that we used to purify the complex plant extract. The automation of injection/collection cycles repeated over several days with this reproducibility could not be possible without the flexibility of the chromatography manager (Empower 2) of the HPLC system. Fig. 2 is therefore the evidence that the strategy of purification of complex extracts on analytical reverse phase C18 is efficient and reliable.

3.4. Fractionation by HPLC of the second batch of 'THIM' extract

With the second batch of 'THIM' extract, samples were fractionated on the same HPLC instrument as previously described but with different conditions. The samples were eluted at 1 ml/min with a gradient of 0.1% glacial acetic acid in water (A), 0.1% glacial acetic acid in MeCN (B), and 100% hexane (C) for post-separation column cleaning. The gradient was as follows: from 55:45:0 A/B/C to 15:85:0 over 35 min with the non-linear gradient curve 7, immediate eluent composition change to 0:100:0, at minute 36 immediate change to 0:0:100 (column cleaning with hexane), at minute 38 immediate change to 0:100:0, isocratic elution until minute 46, linear gradient to 55:45:0 at minute 47. Hexane shows very limited solubility (5–10%) in MeCN (acetoni-

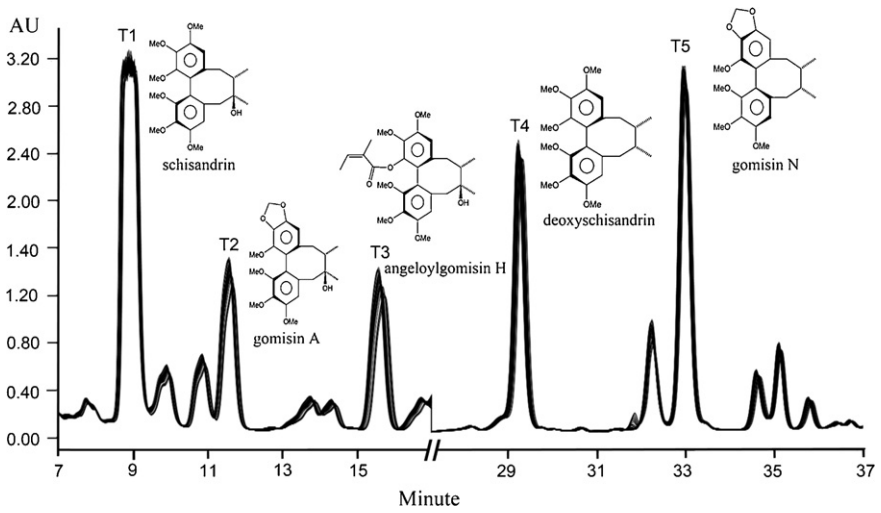

Fig. 2. Overlay of partial chromatograms of Schisandra berries THIM extract, first batch and chemical structures of selected peaks. HPLC conditions are described in Section 3. Chromatograms were extracted at 220 nm. The chemical structure of each peak was determined by NMR/mass spectrometry.

trile) at room temperature, therefore, its use is not common on RP C18 columns. In this step, addition of hexane to the HPLC separation procedure was preferred over adding another cleaning step to the extract preparation since the low solubility was sufficient to remove remaining traces of hexane from the column during 100% MeCN re-conditioning (minute 38–46). Hexane also happened to be efficient in removing unwanted materials such as chlorophyll or fatty acids strongly retained by the RP C18 stationary phase. Immediate eluent composition changes were achieved using gradient curve 1. Re-equilibration time was 10 min, and each sample set started with a blank injection. The plant extract was dissolved in the starting mobile phase (55:45:0, A/B/C) and 30 μl of saturated solution was the typical injection volume. These improved conditions along with the automated injection/collection cycles enabled to achieve a separation of 3–18 mg of pure compounds over a 96-h period without a significant decrease in the purity of the targeted peaks (degree of purity >95%) as assessed by tandem HPLC/NMR under the conditions described in Section 2 for the NMR.

The chromatogram (Fig. 3) of this second batch shows a slight increase in the overall peak number, as compared to the full chromatogram of batch 1, which may result from the improved HPLC conditions. The fractions were dried, weighed and analyzed by TLC with cerium sulfate charring.

As described in Fig. 2, the chromatogram of the second batch was also extracted at 220 nm and the compound identifications were achieved by NMR and mass spectrometry. Tandem HPLC/NMR analysis confirmed the targeted peaks to be >95% pure. The peak cluster eluting from the 17th to the 25th minute was twice less active than the parent THIM extract, and was not further separated. Table 1 summarizes the results of the HPLC separation of the two batches. Although conditions were optimized in the second batch, there was no significant difference in the peak numbers and their elution times.

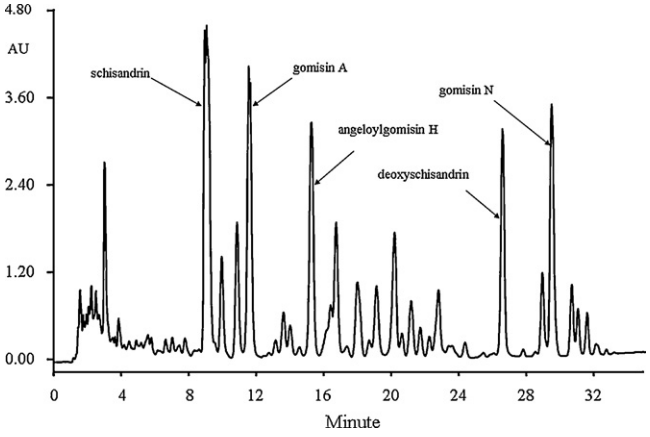

Fig. 3. Chromatogram of Schisandra berries THIM extract, second batch and peak identity. HPLC conditions are described in Section 3.

Once the structures of the compounds were identified, their anti-proliferative activity in the bioassay were compared on a molar basis, as shown in Fig. 4. The concentrations inhibiting cell growth by 50% (IC_{50}) were determined from the dose–response curves and were the following: gomisin A, 716 μM; angeloylgomisin H, 696 μM; deoxyschisandrin, 336 μM; gomisin N, 43 μM. Schisandrin was devoid of detectable activity.

Table 1
Summary of two analytical reverse phase HPLC fractionations of extract from the berries of *S. chinensis*.

Compound	Initial HPLC fractionation	48 h period	Optimized HPLC fractionation		96 h period
	Elution time (min)	Dry weight (mg)	Elution time (min)	Dry weight (mg)	Activity[a] IC_{50} (μg/ml)[b]
Extract					136
Schisandrin	9.0	3.1	9.0	17.8	>1000
Gomisin A	11.5	1.6	11.5	5.4	300
Angeloylgomisin H	15.5	1.1	15.5	3.7	348
Deoxyschisandrin	29.5	1.4	26.5	2.7	140
Gomisin N	33.0	1.2	29.5	3.0	17

[a] Activity was determined in the human colorectal carcinoma cell line HT29 using the MTS cell viability assay.
[b] IC_{50} values were derived from sigmoidal dose–response curves. Values are the average of two independent experiments performed in triplicate.

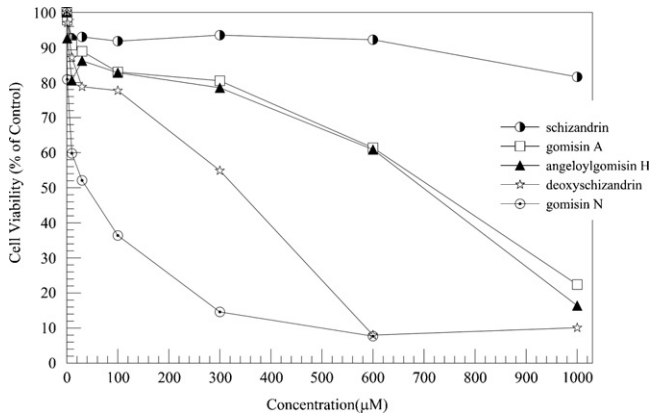

Fig. 4. Comparative activities of the purified constituents of Schisandra berries on the human colorectal cancer cell line HT-29. Each point represents the average of six determinations from two separate experiments run in triplicate.

3.5. Insight into the structure–activity relationships of the compounds

The mechanism underlying the anti-proliferative activity of these lignans on their molecular target in human colorectal cancer is unknown. The current results were obtained in a single cultured cancer cell line (HT-29), but reveal consistent structural determinants for the activity of these molecules as shown in Fig. 5.

A comparison of Schisandrin with deoxyshisandrin shows that the 7-OH group in Schisandrin reduces the activity. A comparison of Schisandrin with gomisin A reveals that a methylenedioxy group between C12 and C13 enhances the activity. In agreement with our findings, Lee et al. showed that lignans from *S. senensis* exerted a greater inhibitory activity of platelet activating factor (PAF) when the molecules lacked a 7-OH [14]. However, a methylenedioxy group in their studies decreased the PAF inhibitory activity, which suggests that the molecule acts on an unrelated molecular target.

Gomisin N, the most active of these five compounds, has both of these activity-enhancing determinants. However, the compound has the opposite twist of the biphenyl ring system (*S*-biphenyl configuration), which changes the shape of the molecule. Min et al. [9], in a similar anti-proliferative study, reported that gomisin N was more active than wuweizisu B, the *R*-biphenyl configured form of gomisin N. Their study utilized a different panel of human cancer cell lines that included the HCT-15 colorectal carcinoma cell line that lacks several chromosomes and does not express the key tumor suppressor p53 protein, thereby complicating the comparison between the two studies. Angeloylgomisin H differs from inactive Schisandrin only by having an angeloyl group at C14, yet it has moderate activity. Angeloylgomisin K_3 which differs from angeloylgomisin H in lacking the 7-OH, was not isolated in our study and reports of its chemical characterization mentioned no activity [15,16]. From our results it would be expected to have greater activity than angeloylgomisin H in our bioassay.

3.6. NMR study of the most active compounds

The two most active fractions T4 and T5, identified as deoxyschisandrin and gomisin-N, respectively, were studied in more detail by 1D and 2D NMR methods than previously reported. The 600-MHz ^{1}H spectrum of T4 showed six resolved methoxy singlets (four near 3.88 ppm and two near 3.59 ppm); two methyl doublets in the upfield region (0.7–1.0 ppm); two aromatic singlets near 6.5 ppm; and two ABX systems with the AB portions in the 2.0–2.6 ppm region and the X portions near 1.8 ppm. The ^{1}H spectrum of T5 was similar, but with only four methoxy peaks and with a new AB pattern near 5.9 ppm with J_{ab} = 1.5 Hz. This indicates that two adjacent methoxy groups in T4 have been replaced with a methylenedioxy (O–CH_2–O) group forming a 5-membered ring in T5. Aside from this one difference, there are striking similarities between T4 and T5 in the ^{1}H and ^{13}C chemical shifts, and in the ^{1}H coupling patterns and *J* values.

Two-dimensional DQF-COSY, HSQC and HMBC spectra at 600 MHz ^{1}H frequency proved the covalent structure of deoxyschisandrin (T4) and gomisin-N (T5). Molecular modeling and prediction of 3-bond H–H and C–H coupling constants confirmed the stereochemistry of the methyl groups in the 8-membered ring as well as the biphenyl "twist" stereochemistry. Comparison of the structures of (+) deoxyschisandrin and (−) gomisin-N (Fig. 6) shows that there is a near mirror-image symmetry, with the only difference being the replacement of the 2-OMe and 3-OMe groups of (+) deoxyschisandrin with the 12,13-O–CH_2–O ring of (−) gomisin-N.

This symmetry is reflected in the ^{1}H shifts and *J*-coupling patterns (Table 2) as well as in the ^{13}C shifts (Table 3), provided that the reversed numbering system of gomisin-N is accounted for in the comparison (e.g., C1 of deoxyschizandrin corresponds to C14 of gomisin-N in Fig. 6).

Table 2
^{1}H chemical shift assignments at 600 MHz for gomisin-N and deoxyschisandrin in $CDCl_3$. Chemical shifts are relative to tetramethylsilane at 0 ppm. Protons in CH_2 groups are designated α for below the plane of the molecule as drawn in Fig. 6 and β for above the plane. Assignments were confirmed by 2D HSQC, DQF-COSY and HMBC.

Gomisin-N			Deoxyschisandrin		
Position	^{1}H ppm	Mult.	Mult.	^{1}H ppm	Position
1-OMe	3.544	s, 3H	s, 3H	3.585	14-OMe
2-OMe	3.893	s, 3H	s, 3H	3.884	13-OMe
3-OMe	3.881	s, 3H	s, 3H	3.888	12-OMe
4	6.549	s, 1H	s, 1H	6.542	11
6α	2.568	dd, 1H, 13.6, 7.3	dd, 1H, 13.5, 7.4	2.581	9α
6β	2.521	dd, 1H, 13.6, 2.2	dd, 1H, 13.5, 1.9	2.502	9β
7	1.888	m, 1H	m, 1H	1.910	8
7-Me	0.732	d, 3H, 7.2	d, 3H, 7.2	0.739	8-Me
8	1.778	m, 1H	m, 1H	1.811	7
8-Me	0.968	d, 3H, 7.2	d, 3H, 7.2	1.001	7-Me
9α	2.223	dd, 1H, 13.3, 9.5	dd, 1H, 13.3, 9.6	2.278	6α
9β	2.020	dd, 1H, 13.3, 1.4[a]	dd, 1H, 13.3, 1.3[a]	2.055	6β
11	6.476	s, 1H	s, 1H	6.534	4
O–CH_2–O	5.941	d, 1H, 1.5	s, 3H	3.899	3-OMe
O–CH_2–O	5.947	d, 1H, 1.5	s, 3H	3.873	2-OMe
14-OMe	3.816	s, 3H	s, 3H	3.589	1-OMe

[a] *J* value estimated from line broadening.

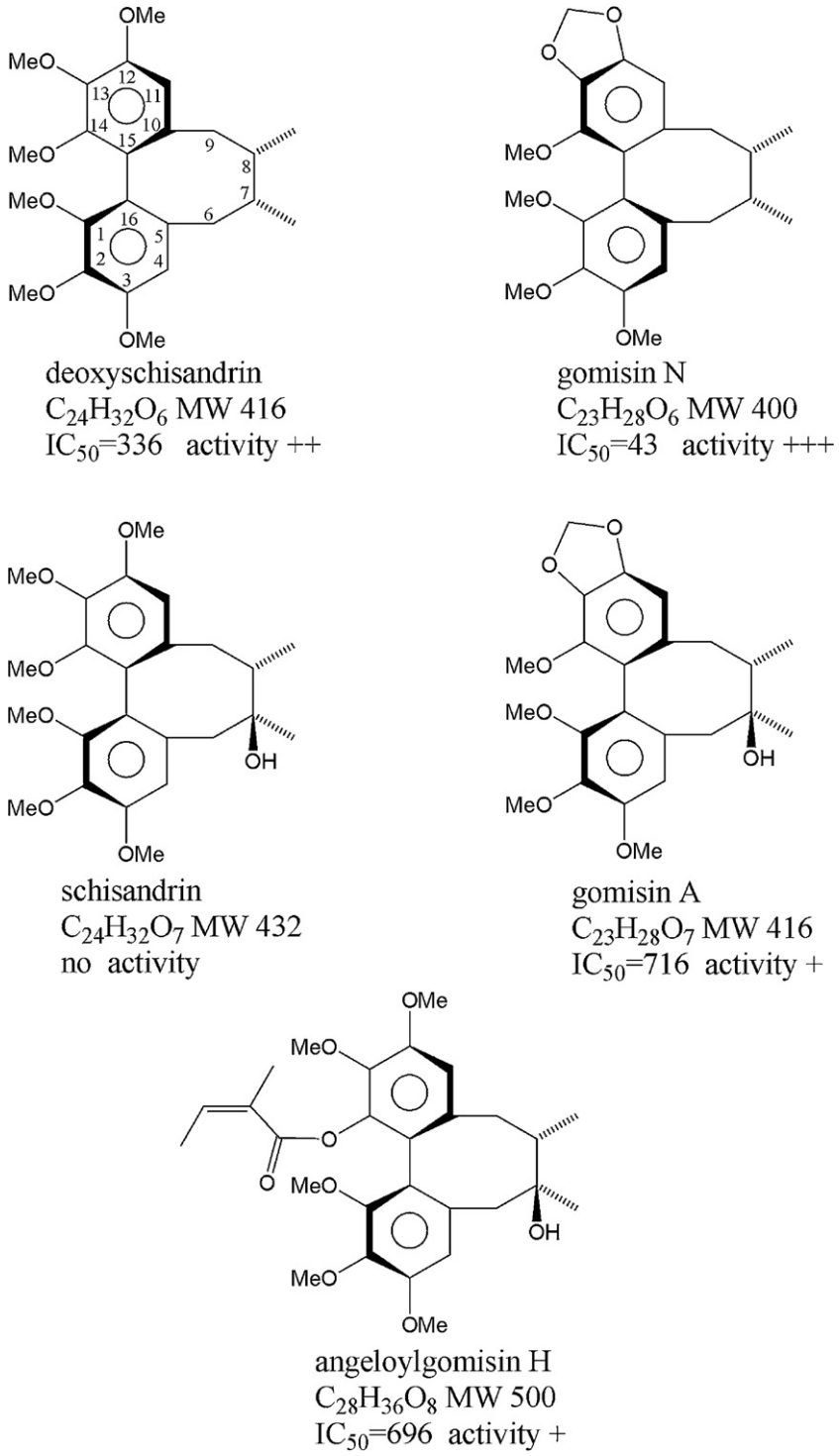

Fig. 5. Structures of the compounds isolated from *S. chinensis* and key structural determinants influencing their anti-proliferative activity on the human colorectal cancer cell line HT-29.

Published ^{1}H NMR data on deoxyschisandrin at 100 MHz [17] and 300 MHz [18] gives only chemical shift values. Only two methoxy chemical shifts are reported and these are not assigned to specific positions. A single chemical shift is given for protons 9α and 9β and for protons 4 and 11. For the 300 MHz data [18] the 6α and 6β protons are assigned a single shift, and the H6/H9 and H7-Me/H8-Me assignments are reversed. Published ^{13}C data on deoxyshisandrin [18] closely match our data (Table 3), except that C2/C13 are reversed and the methoxy carbons are not specifically assigned. There are no published or deposited X-ray coordinates for deoxyschisandrin.

Gomisin-N has better structural characterization in the literature. The reported 100 MHz proton data [17] show only three methoxy signals, without assignment, a single shift for H6α/H6β and for H7/H8, and the H4 and H11 assignments are backwards. Data reported at 400 MHz [19] correctly differentiate the H7 and H8 peaks, but the H9α and H9β assignments are reversed. In both cases, *J* couplings are reported only for the doublet methyl

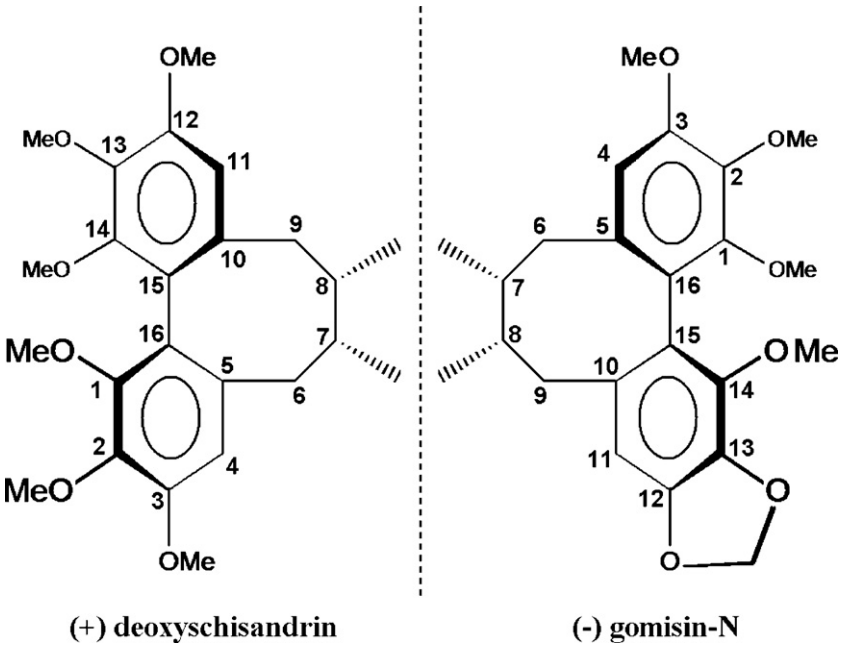

Fig. 6. Structures of (+) deoxyschisandrin and (−) gomisin, with carbon numbering. The dotted line represents a plane of near-symmetry, broken only by the replacement of 2,3-dimethoxy in deoxyschisandrin by the 12,13-methylenedioxy in gomisin-N.

groups and for H9α and H9β. In particular, the position 9 coupling data match ours (Table 2) very well (13.5/8 Hz and 13.5/1 Hz [17]; 13.2/9.2 Hz and 13.2 br. d. [19]). A more recent report [20] of 400 MHz ^{1}H data shows *J* couplings only for the doublet methyl groups, whose assignments are reversed. NMR data at 500 MHz ^{1}H frequency were reported [21] in CD_3OD for deoxyschisandrin and in $CDCl_3$ for gomisin-N. The deoxyschisandrin ^{13}C shifts match our data (average $\Delta\delta = 0.25$ ppm, std. dev. 0.03), except for reversed assignments of C2/13 and C1/14 and a typographic error for C12. *J* coupling values for the deoxyschisandrin AB(X) systems are similar to ours, but assignments are not stereospecific ("6a" 13.5/2.0 Hz and "6b" 13.5/7.5 Hz). An X-ray crystal structure [22] is available for gomisin-N.

Our stereospecific assignments are based on the X-ray structure of gomisin-N and an energy-minimized model of deoxyschisandrin. Fig. 7 shows a view of the gomisin-N structure with C16 directly behind C9 and C15 directly behind C10. The calculated deoxyschisandrin structure is essentially the mirror image of this structure, with corresponding numbering as shown in Tables 2 and 3.

Dihedral angles from the H7 proton to H6α/H6β and from the H8 proton to H9α/H9β of gomisin-N are shown, with nearly orthogonal dihedrals corresponding to the small vicinal H–H couplings observed (89° angle, $J_{8-9\beta}$ not resolved; 70° angle, $J_{7-6\beta}$ 2.2 Hz). Similar results were seen with the calculated deoxyschisandrin structure (91° angle, $J_{7-6\beta}$ not resolved; 68° angle, $J_{8-9\beta}$ 1.9 Hz). Dihedral angles for 3-bond C–H couplings correspond well with the observed intensities of HMBC crosspeaks. For gomisin-N, the H9β-C8Me (28°) and H6β-C7Me (171°) crosspeaks are clearly observed but the H9α-C8Me (89°) and H6α-C7Me (74°) are missing.

Table 3
^{13}C chemical shift assignments at 600 MHz for gomisin-N and deoxyschisandrin in $CDCl_3$. Chemical shifts are relative to solvent $CDCl_3$ at 77.0 ppm. Assignments were confirmed by 2D HSQC, DQF-COSY and HMBC.

Gomisin-N			Deoxyschisandrin		
Position	Lit. [18]	^{13}C ppm	^{13}C ppm	Lit. [20]	Position
1	151.6	151.59	151.50	151.62	14
1-OMe	60.5	60.55	60.54	60.74	14-OMe
2	140.0	139.99	140.03	139.97	13
2-OMe	61.0	61.01	60.95	61.17	13-OMe
3	151.5	151.52	151.56	153.09	12
3-OMe	55.8	55.86	55.87	56.12	12-OMe
4	110.6	110.58	110.43	110.74	11
5	134.1	134.08	133.90	134.17	10
6	39.1	39.10	39.13	39.37	9
7	33.5	33.53	33.74	33.98	8
7-Me	12.8	12.82	12.65	12.88	8-Me
8	40.7	40.69	40.75	41.00	7
8-Me	21.6	21.56	21.81	21.99	7-Me
9	35.4	35.48	35.57	35.82	6
10	137.8	137.81	139.14	139.40	5
11	102.9	102.94	107.12	107.43	4
12	148.6	148.62	152.83	153.09	3
O–CH_2–O	100.7	100.71	55.90	56.12	3-OMe
13	134.5	134.51	139.69	140.32	2
–	–	–	60.93	61.17	2-OMe
14	141.0	141.00	151.37	151.75	1
14-OMe	59.6	59.63	60.54	60.74	1-OMe
15	121.3	121.30	122.29	122.57	16
16	123.2	123.25	123.34	123.62	15

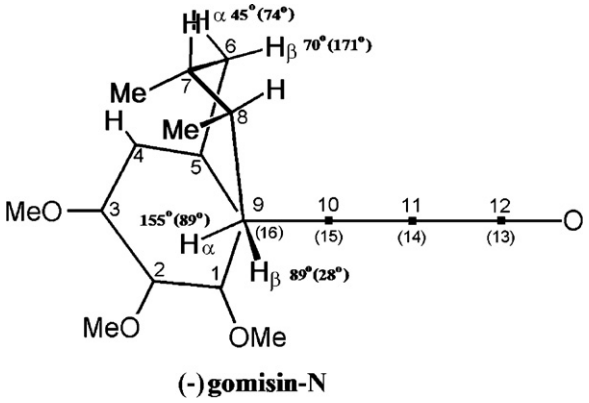

Fig. 7. View of gomisin-N X-ray crystal structure [21] with C9-C10-C15-C16 plane edge-on and C15 and C16 directly behind C10 and C9, respectively. The C1–C5, C16 aromatic ring is in the background, below H9α. Dihedral angles are shown for H6–H7 (H6–C7Me) and for H9–H8 (H9–C8Me).

Likewise for deoxyschisandrin, the H6β-C7Me (21°) and H9β-C8Me (179°) are strong but the H6α-C7Me (92°) and H9α-C8Me (71°) are missing. In every case (16 selected HMBC crosspeaks for each compound), the relative intensity of the gomisin-N HMBC crosspeak correlated very closely with that of the pseudosymmetry-related deoxyschisandrin crosspeak. The strong correlations between dihedral angle and $^3J_{HH}$ or HMBC crosspeak intensity confirm the relative stereochemistry of the two methyl-bearing carbons (C7 and C8) and of the biphenyl twist (C5–C16–C15–C10) in both compounds.

4. Conclusions

The results of the current study show that many of the active constituents of Schisandra fruit extract can be isolated by analytical HPLC in milligram amounts, enabling both structure elucidation and pharmacological testing. For years, analytical HPLC has been the reference method for the quantitative and qualitative analysis of the contents of complex mixtures. This method has been useful in purifying most of the constituents of Schisandra berries [4]. Under the experimental conditions developed in this study, 1–20 mg of pure benzocyclooctadiene lignans were isolated from the Schisandra fruit extracts by continuous unattended operating reversed phase HPLC for 2–4 days. Because of the increased resolution of this analytical technique, the method described herein may supersede standard semi-preparative methods for the separation of complex mixtures.

NMR methods and spectrometers are constantly improving, yielding higher resolution and more precise correlations. The 600 MHz data for gomisin-N and deoxyschisandrin clarify some errors and disagreements in the literature and add new information on dihedral angles. Both measured H–H coupling constants and HMBC crosspeak intensities, which are related directly to H–C coupling constants, can be used to test conformation and stereochemistry in structural models. The solution NMR data are consistent with the X-ray crystal structure of gomisin-N, as well as with the calculated structure of deoxyschisandrin. In addition, ^{1}H chemical shifts could be stereospecifically assigned for the two aliphatic methylene groups of each compound.

Colorectal carcinoma is the third leading cause of mortality in the industrialized nations with more than half a million deaths a year [23] and the rate is steadily on the rise. Most relevant to the current studies targeted at this disease is the recent introduction of Schisandra berries into food, drink and pastry (www.organicchiberry.com). However, the most active constituents, deoxyschisandrin and gomin N, represent only about 33 mg/100 g of dry fruit. Given this minute amount, it is unknown whether the daily consumption of the fruit pastry or drink can provide a significant preventive measure against colorectal proliferative processes.

Current anti-cancer drug development requires compound leads to be within the tenth of micromolar ranges of potency. Nearly five-dozen compounds have been isolated from Schisandra berries [4] and most have been assigned a myriad of pharmacological activities [1]. However, the clinical application of these compounds has been thwarted by their lack of high potency (very low IC_{50s}) and specificity. The relatively high IC_{50} values of gomisin N, the most promising compound of Schisandra fruits, mitigate against its clinical development. Nevertheless, the structure–activity relationships of the molecule on its molecular cellular target suggest that gomisin N may serve as a chemotype for anti-colorectal cancer drug development. It is also possible that refinement of analytical and chromatographic techniques will enable the resolution of new molecules from Schisandra with higher potency and specificity which will translate into clinical success.

Acknowledgments

We acknowledge Dr. Pierluigi Delmonte (U.S. Food and Drug Administration, College Park, MD) for helpful discussions regarding the optimization of the chromatographic separation and fractionation.

We are also grateful to Dr. David Mold for his reading and comments on the manuscript.

References

[1] A. Panossian, G. Wikman, J. Ethnopharmacol. 118 (2008) 183.
[2] Chinese Pharmacopoeia Commission, Pharmacopoeia of the People's Republic of China, vol. 1, People's Medical Publishing House, Beijing, 2005, p. 109.
[3] H. Wagner, R. Bauer, Chinese Drug Monographs and Analysis: Fructus Schisandrae, Wuweizi 1, No. 4, 1996, p. 1.
[4] Y. Lu, D.-F. Chen, J. Chromatogr. A 1216 (2009) 1980.
[5] N.K. Kochctkov, A. Khorlin, O.S. Chizhov, V. Sheichenko 1, Tetrahedron Lett. 31 (1961) 730.
[6] S.Y. Yim, Y.J. Lee, Y.K. Lee, S.E. Jung, J.H. Kim, J.E. Kim, H.J. Kim, B.G. Son, Y.H. Park, Y.G. Lee, Y.W. Choi, D.Y. Wang, Mol. Med. Rep. 2 (2009) 725.
[7] L. Li, Q. Lu, Y. Shen, X. Hu, Biochem. Pharmacol. 71 (2006) 584.
[8] K. Yasukawa, Y. Ikeya, H. Mitsuhashi, M. Iwasaki, M. Aburada, S. Nakagawa, M. Takeuchi, M. Takido, Oncology 49 (1992) 68.
[9] H.-Y. Min, E.-J. Park, J.-Y. Hong, Y.-J. Kang, S.-J. Kim, H.-J. Chung, E.-R. Woo, T.M. Hung, U.J. Youn, Y.S. Kim, S.S. Kang, K. Bae, S.K. Lee, Bioorg. Med. Chem. Lett. 18 (2008) 23.
[10] Y.J. Lee, J.Y. Cho, J.-H. Kim, W.-K. Park, D.-K. Kim, M.-R. Rhyu, Biol. Pharm. Bull. 27 (2004) 1066.
[11] A. Espada, A. Marin, C. Anta, J. Chromatogr. A 1030 (2004) 43.
[12] Z. Lou, H. Zhang, C. Gong, Z. Zhu, L. Zhao, Y. Xu, B. Wang, G. Zhang, Rapid Commun. Mass Spectrom. 23 (2009) 831.
[13] P. Shi, Q. He, Y. Zhang, H. Qu, Y. Cheng, Phytochem. Anal. 20 (2009) 197.
[14] I.S. Lee, K.Y. Jung, S.R. Oh, S.H. Park, K.S. Ahn, H.-K. Lee, Biol. Pharm. Bull. 22 (1999) 265.
[15] C. Lei, S.-X. Huang, J.-J. Chen, J.-X. Pu, L.-B. Yang, Y. Zhao, J.-P. Liu, X.-M. Gao, W.-L. Xiao, H.-D. Sun, Chem. Pharm. Bull. 55 (2007) 1281.
[16] H.-M. Li, Y.-M. Luo, J.-X. Pu, X.-N. Li, C. Lei, R.-R. Wang, Y.-T. Zheng, H.-D. Sun, R.-T. Li, Helvetica Chim. Acta 91 (2008) 1053.
[17] Y. Ikeya, H. Taguchi, I. Yosioka, H. Kobayashi, Chem. Pharm. Bull. 27 (1979) 2695.
[18] S.-J. Jiang, Y.-H. Wang, D.-F. Chen, Zhongguo Tianran Yaowu 3 (2005) 78.
[19] H. Tang, Y. Yi, X. Yao, Q. Xu, S. Zhang, P. Sun, Zhongguo Haiyang Yaowu 21 (2002) 11.
[20] H. Iwata, Y. Tezuka, S. Kadota, A. Hiratsuka, T. Watabe, Drug Metab. Dispos. 32 (2004) 1351.
[21] S.-M. Seo, H.-J. Lee, Y. Park, M.K. Lee, J.-I. Park, K.-H. Paik, Nat. Prod. Sci. 10 (2004) 104.
[22] J. Marek, J. Slanina, Acta Crystallogr., Sect. C 54 (1998) 1548 (Cambridge Crystallographic Database POVM1W).
[23] D.M. Parkin, Lancet Oncol. 2 (2001) 533.